Fermi National Accelerator Laboratory

FERMILAB-Conf-90/275

Low Energy Aspects of Circular Accelerators *

Stephen D. Holmes
Fermi National Accelerator Laboratory
P.O. Box 500
Batavia, Illinois 60510

December 1990

* Lecture given at the 1990 US-CERN School on Particle Accelerators, Topical Course on Frontiers of Particle Beams: Intensity Limitations, Hilton Head, South Carolina, November 7-14, 1990.

Operated by Universities Research Association Inc. under contract with the United States Department of Energy

LOW ENERGY ASPECTS OF CIRCULAR ACCELERATORS

Stephen D. Holmes
*Fermi National Accelerator Laboratory**
P.O. Box 500
Batavia, Il. 60510

1. Introduction

Performance in circular accelerators can be limited by some of the same sorts of phenomona described by Miller[1] and Wangler[2] in their lectures on low energy behavior in linear accelerators. In general the strength of the perturbation required to degrade performance is reduced in circular accelerators due to the repetetive nature of the orbits. For example, we shall see that space-charge can severely limit performance in circular accelerators even when operating far from the "space-charge dominated regime" as defined in linear accelerators.

We will be discussing two particular aspects of low energy operation in circular accelerators--*space-charge* and *transition*. "Low energy" is defined within the context of these phenomona. We shall see that the phenomona are really only relevant in hadron accelerators. First, for space-charge the low energy regime is given approximately by,

$$\gamma^2 \lesssim \frac{N_p r_p}{\varepsilon_N}\left(\frac{Z^2}{A}\right) .$$

Here γ is the relativistic factor of the beam, N_p is the total number of particles in the accelerator, r_p is the classical radius of the proton, ε_N is the transverse normalized beam emittance, and Z and A are the particle charge and atomic weight. Circular accelerators which operate in this regime are typically the initial circular ring in a hadron accelerator complex. Examples include the Fermilab, CERN, and Brookhaven Boosters, the Brookhaven AGS, the SSC Low Energy Booster, various KAON Factories, and, perhaps surprisingly, the CERN S$\bar{p}$pS[3]. The primary impact of space-charge is to limit the transverse phase space densities which can be delivered from these machines. This is obviously of vital importance in hadron colliders where luminosity is directly proportional to transverse phase space density.

* Operated by Universities Research Association under contract with the U.S. Department of Energy

Transition crossing takes place in accelerators in which the beam attains the condition

$$\gamma^2 = \frac{R}{<\eta>}$$

sometime during the acceleration cycle. Here R is the average radius of the machine and $<\eta>$ is the average dispersion function in the bending magnets. Such a condition has no analog in linear accelerators and is again typically encountered in the injector stages of hadron accelerator complexes. Examples here include the Fermilab Booster and Main Ring, the Brookhaven AGS and the Relativistic Heavy Ion Collider (RHIC), the CERN PS, and, potentially, the SSC Low and Medium Energy Boosters. In contrast to space-charge, transition is primarily a longitudinal effect which can limit one's ability to accelerate high intensity beams. It is important in any accelerator complex which either contains a longitudinal bottleneck, or one in which short bunch length is important, e.g. in a collider with non-zero crossing angle.

2. Space-Charge

We will start by examining data obtained in the Fermilab Booster[4] as displayed in Figure 1. The figure shows the beam emittance delivered from the Booster as a function of beam intensity. The emittance displayed here is the *95% normalized transverse emittance*. The relationship between the beam emittance (ε_N), beam sigma (σ), lattice function (β_L), and relativistic factors (γ and β) is given by,

$$\sigma = \sqrt{\frac{\varepsilon_N \beta_L}{6\pi\beta\gamma}} \quad . \qquad (1)$$

The data show a dependence of the delivered emittance on the delivered intensity of the form,

$$\varepsilon_N/\pi \text{ (mm-mr)} = \text{Max}(7, 6N_p \times 10^{-12})$$

where N_p is the total number of particles delivered. The maximum number of particles delivered is 3.3×10^{12} and corresponds to an emittance of 20π mm-mr--the aperture of the machine at the injection energy of 200 MeV. Since the Booster utilizes an H^- multi-turn injection, the emittance should, in principle, be independent of the intensity. The observed correlation is believed to be due to space-charge forces at injection into the Booster.

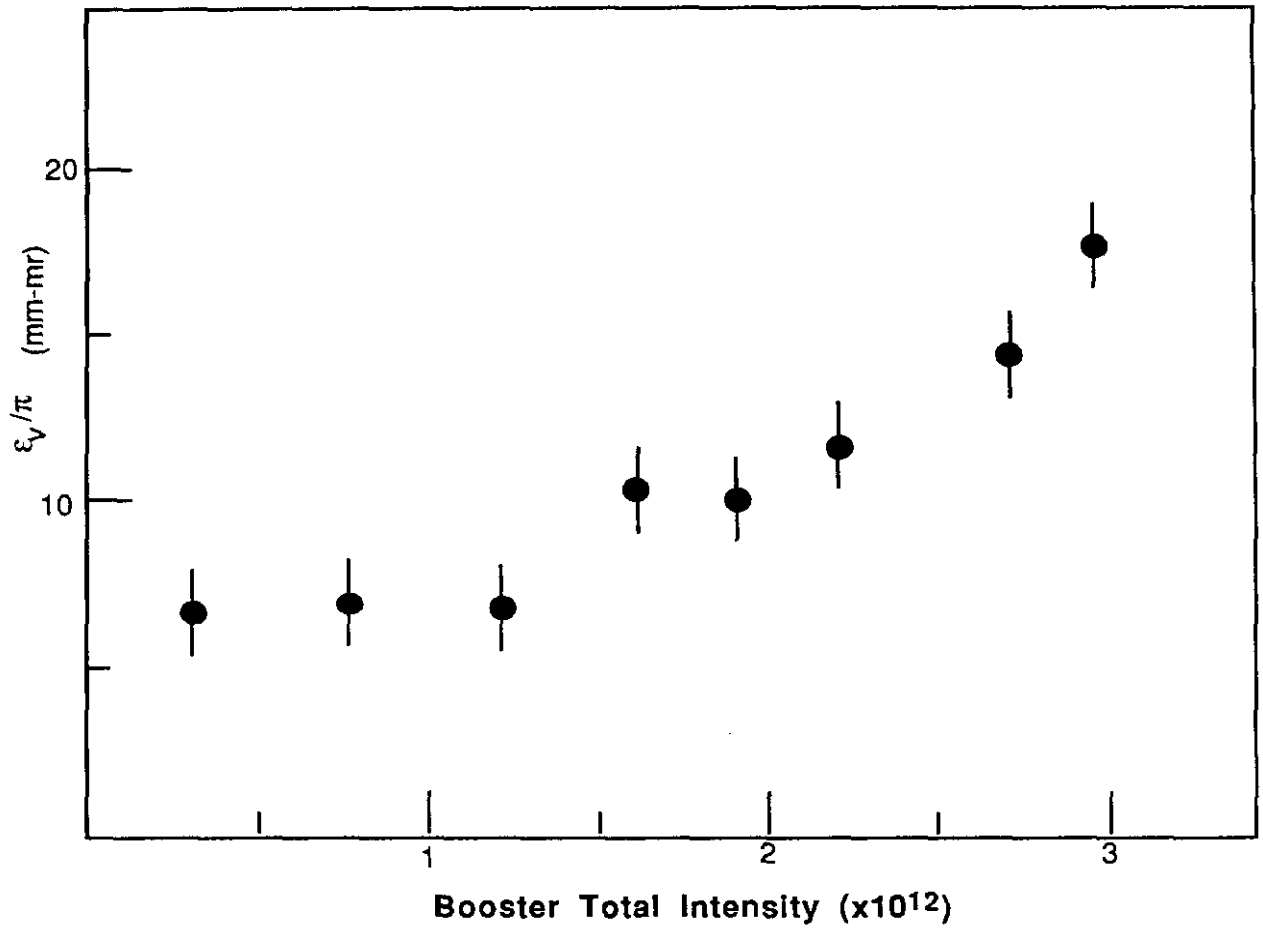

Figure 1: Transverse emittance delivered from the Fermilab Booster as a function of beam intensity.

The data shown in Figure 1 can be interpreted in terms of the Laslett tune-shift[5]. The Laslett formula relates the detuning in a circulating charged particle beam to basic beam intensity and kinematic parameters. Consider a bunch of charged particles (we assume q=e here) of length L, moving with a common velocity v, as shown in Figure 2. In order to simplify the discussion we will, for the moment, assume a uniform charge distribution, and will let R be the radius and N the total number of protons in the bunch. The electric field seen by a comoving proton a distance r off axis is given by Gauss' Law:

$$\vec{E} = \frac{eN}{2\pi\varepsilon_0 L R^2}\ \vec{r}\ .$$

Likewise, the magnetic field is,

$$\vec{B} = \frac{v}{c^2}\,|\vec{E}\,|\,\hat{\phi}.$$

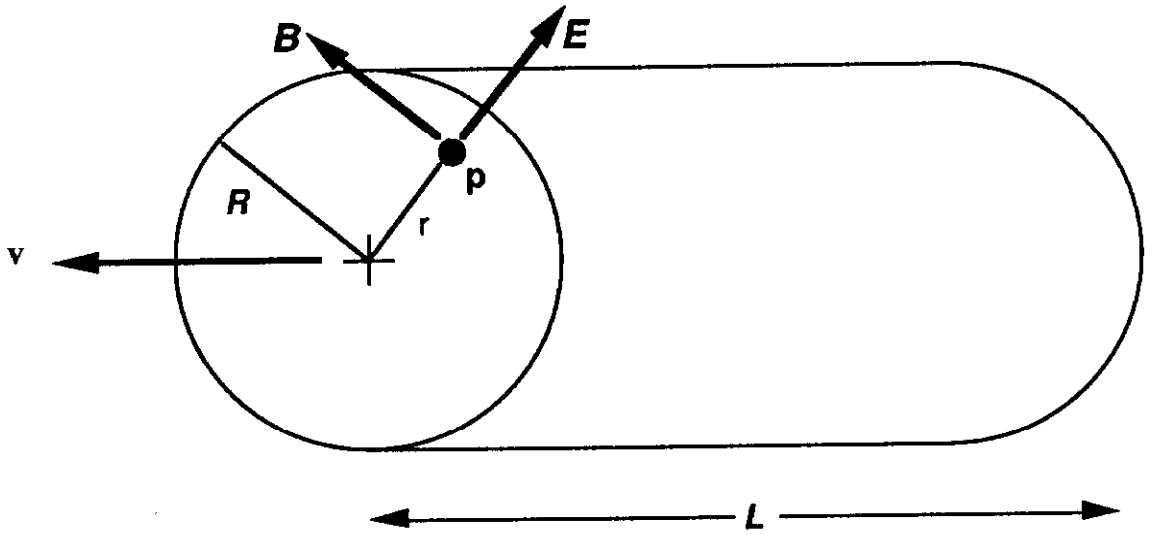

Figure 2: The electric and magnetic fields seen by a proton comoving at a velocity v with a bunch of length L and radius R, containing N protons.

The force experienced by the proton is then given by,

$$\vec{F} = e\vec{E} + \vec{v}x\vec{B} = \left(\frac{e^2N}{2\pi\varepsilon_o LR^2}\right)(1-\beta^2)\ \vec{r}\ .$$

Note that the force is linear in the displacement r and defocussing in nature. The effect on the proton is the same as that of a quadrupole with a strength parameter, k (=B'/(Bρ)), of

$$k=-\left(\frac{e^2}{2\pi\varepsilon_o mc^2}\right)\frac{N}{LR^2}\frac{1}{\gamma^3\beta^2} = \frac{2r_pN}{LR^2}\frac{1}{\gamma^3\beta^2}.$$

The tune shift due to a perturbation, Δk, over a distance l is given by,

$$\Delta\nu = \frac{\beta_L \Delta k l}{4\pi}$$

where β_L is the lattice beta at the position of the perturbation. So for a complete traversal of the accelerator, the tune shift seen by the proton is,

$$\Delta\nu = -\frac{\beta_L r_p}{2\pi R^2\gamma^3\beta^2}\left(\frac{NC}{L}\right). \qquad (2)$$

Here C is the total circumference of the accelerator.

Note that the tune shift is independent of r under the assumption of a uniform charge distribution. In reality the charge distribution is more like a Gaussian in the transverse coordinates,

$$\frac{dN}{dxdy} = \frac{N}{2\pi\sigma^2} \exp\left(\frac{-(x^2+y^2)}{2\sigma^2}\right).$$

So we can easily write the tune shift experienced by protons near the center of the beam by making the replacement $\pi R^2 \rightarrow 2\pi\sigma^2$ in (2) and use equation (1) to express in terms of the emittance. We will also change from particles per bunch, N, to total particles, N_p, by rewriting the quantity (NC/L) as (N_p/B) where B is called the "bunching factor".

$$\boxed{\Delta\nu = -\frac{3r_pN_p}{2\varepsilon_N\beta\gamma^2B}} \qquad (3)$$

Equation (3) is the Laslett tune shift formula. It gives the detuning of particles near the (transverse) center of the bunch. The tune shift is incoherent in the sense that different particles in the beam experience different tune shifts with large betatron amplitude particles experiencing no shift at all, i.e. $\Delta\nu$ is really a *tune spread*. The tune shift as a function of betatron amplitude has been given by Evans[6] in a previous accelerator school, and the interested reader is referred to those proceedings. In addition to the transverse dependence, if the longitudinal charge distribution is non-uniform a particle will experience a tune shift which is modulated at twice the synchrotron frequency as it travels through regions of varying charge density. There can also be coherent contributions to the tune shift arising from image currents/charges in the vacuum chamber. In general these are small compared to the incoherent tune shift for bunched beams and will be ignored here.

2.1 Observations

It has been observed in existing proton accelerators that there appears to be a limit on how large a $\Delta\nu$ can be obtained. For example the linear increase of transverse emittance with intensity in the Fermilab Booster shown in Figure 1 corresponds to a tune shift $\Delta\nu = 0.4$ at the injection energy of 200 MeV. Other accelerators such as the Brookhaven AGS and the CERN PS Booster have attained $\Delta\nu$'s in the range 0.5-0.8. Note that in addition to limiting the phase space density achievable, for an accelerator with a given aperture, any limit imposed upon N_p/ε_N also translates into a limit on total intensity. It is believed today that

the limit on acheivable $\Delta\nu$'s represents the most fundamental intensity limit in low energy proton synchrotrons.

The following characteristics of equation (3) should be noted: First, the space-charge tune shift is proportional to the total charge in the accelerator. In particular this means that smaller circumference rings can support higher line charge densities for the same value of $\Delta\nu$. Such reasoning has provided the impetus for the construction of the AGS Booster, and for the inclusion of the SSC Low Energy Booster into the SSC injector design. Second, the kinematic factor, $\beta\gamma^2$, in the denominator of (3) insures that space-charge is usually significant only at injection energy into the lowest energy circular accelerator in a hadron accelerator complex. Finally, (3) provides a prescription for curing an accelerator suffering from a space-charge limit--raising the injection energy. This reasoning has provided the impetus for raising the Fermilab Booster injection energy from 200 MeV to 400 Mev through the Fermilab Linac Upgrade, for the choice of 600 MeV for the SSC Linac energy, and again for construction of the AGS Booster.

In the spring of 1990 a series of measurements were completed in the Fermilab Booster to understand in greater detail how the beam emittance becomes diluted to create the correlation observed in Figure 1. Beam profiles were measured for a wide range of beam intensities at times varying between 40 and 3000 μs after injection. (The revolution period at injection is about 2.8μs.) Representative results are shown in Figures 3 and 4. Figure 3 shows beam profiles measured 1000μs after injection for six different beam intensities varying between 4×10^{11} and 3×10^{12}. The increase in beam width with intensity is observed as is a change in the distribution shape. The data have been analyzed in terms of 38%, 68%, and 95% emittances. Figure 4 shows the time evolution of the emittance for an intensity of 2×10^{12}. The following conclusions were drawn:

1. Any beam blowup appears to occur within the first twenty revolutions of the accelerator.

2. The beam profile changes with the core being affected more than the tails.

3. The degree of blowup depends weakly on the bare tune of the machine over the range 6.6 to 6.9.

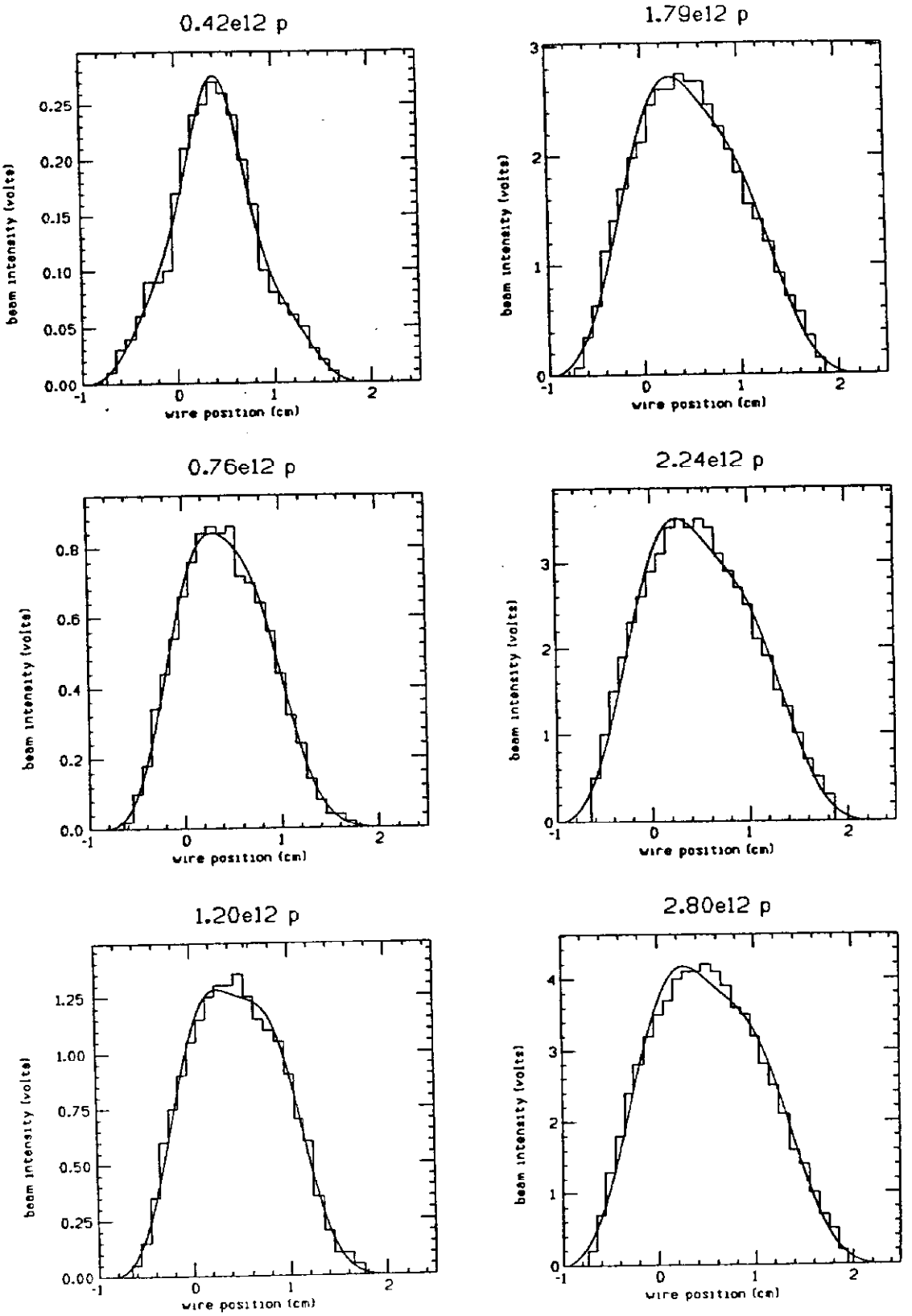

Figure 3: Beam profiles measured in the Fermilab Booster 1msec after injection for a range of beam intensities.

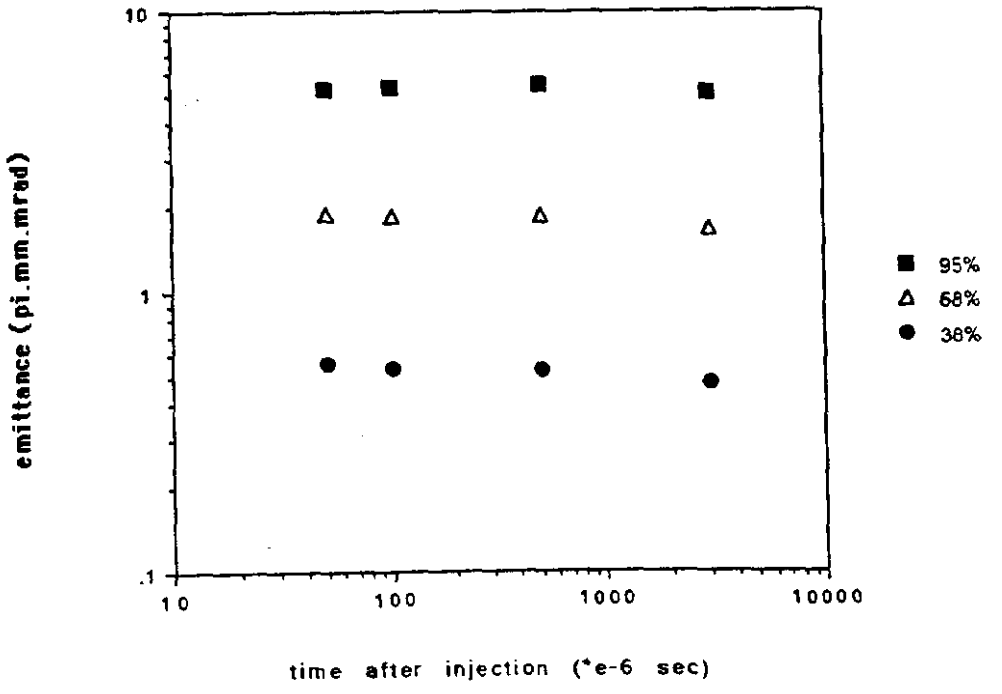

Figure 4: Time evolution of the 38%, 68%, and 95% (unnormalized) transverse emittance for 2×10^{12} protons (2.5×10^{10}/bunch) injected into the Fermilab Booster.

2.2 Phenomonological Descriptions

The question naturally arises, "Whence the limit?" For sometime people have felt that the limit was connected with overlap of the beam with low order machine resonances. Qualitatively this reasoning goes as follows: Since $\Delta\nu$ is really a tune spread, and clearly the half and integer resonances need to be avoided, then the largest $\Delta\nu$ tolerable must lie in the range 0.5 to 1.0, depending upon the selection of the bare tune. Obviously such a statement does not represent a very deep understanding. However, it has provided a criterion for designing new accelerators which are potentially space-charge limited, as long as one designs to a $\Delta\nu$ on the conservative side.

More recently the problem has been attacked using computer tracking simulations[7,8,9,10,11]. The codes have become increasingly sophisticated over the last five years, and now typically track thousands of macroparticles over a few thousand turns incorporating machine imperfections, but not sychrotron oscillations.

Among the more advanced simulations are those of Machida[10] . Machida simulated the SSC Low Energy Booster in a self-consistent manner using 2000 macroparticles tracked with space-charge kicks applied 100 times per revolution. Machida is able to reproduce the characteristic emittance growth with intensity as shown in Figure 5. The $\Delta\nu$ represented here is in the range 0.3 to 0.4. He also investigated the time evolution of the emittance, the dependence upon the bare tune, and the effect of machine errors driving second and third order resonances.

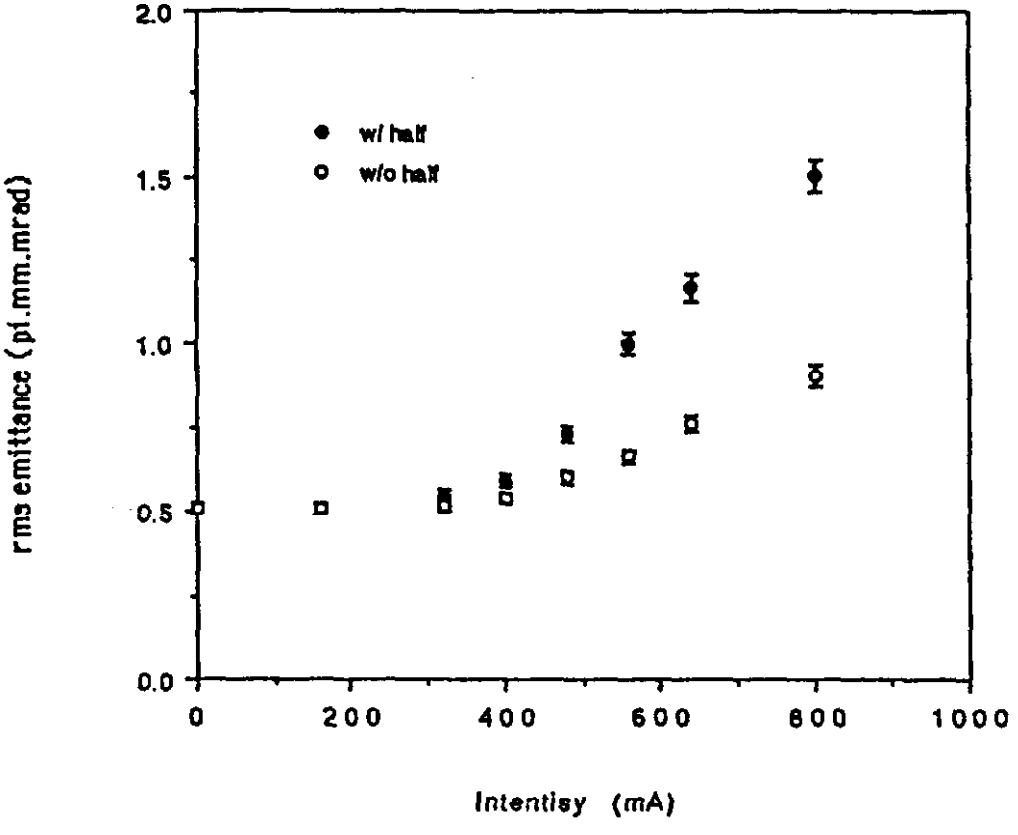

Figure 5: Transverse emittance as a function of beam intensity from the SSC Low Energy Booster simulation of Machida.

Among the conclusions drawn from the simulations are:

1. Emittance dilution is very fast, occuring typically in tens of turns. (Note that this conclusion justifies the exclusion of synchrotron oscillations from the simulations.)

2. Machine imperfection resonances other than the half and integer are irrelevant.

3. Location of the bare tune with respect to the half-integer can change achievable $\Delta\nu$'s by 50%.

4. Dilution is caused by the non-linear fields of the beam itself. In particular the fourth order resonance appears to be important. As a corrolary intrinsic resonances are important and machine tunes approximating $4\nu = nS$ need to be avoided. (S is the superperiodicity of the accelerator. This point is particularly emphasized by both Parzan and Machinda.)

Conclusion 1 is in obvious agreement with the observations described above.

It is worth mentioning that alternative descriptions, not described here, based on envelope equations potentially provide an alternative avenue toward understanding the behavior of circulating beams under the influence of space-charge[12].

3. Transition

The primary concern in hadron accelerators in which the beam is required to pass through transition during the acceleration cycle is longitudinal emittance growth, possibly accompanied by beam loss. Beam loss can occur if either the longitudinal emittance becomes larger than the rf bucket area, or the product of the dispersion times the momentum spread becomes larger than the physical aperture of the accelerator.

One could reasonably ask at this point what difference, in the absence of beam loss, dilution of the longitudinal phase space could make since there is not an obvious connection to collider luminosity as in the case of transverse emittances. At Fermilab the proton beam passes through transition in both the 8 GeV Booster and in the Main Ring, and will likely cross transition in the proposed Main Injector accelerator. The luminosity in the Tevatron proton-antiproton collider is sensitive to the preservation of longitudinal phase space in at least two respects: First, the antiproton production uses a bunch rotation scheme in the Main Ring, followed by debunching of the secondary antiproton beam in the

Debuncher Ring. With this $\bar{p}$ production technique the production rate is nearly proportional to N_p/ε_L, where N_p is the number and ε_L the longitudinal emittance of the targeted, 120 GeV, protons. Second, both proton and antiproton bunches in the collider are created using a longiudinal bunch coalescing method. The efficiency of this operation, and hence the intensity of the bunches formed in the collider, is sensitive to the longitudinal emittance of the pre-coalesced bunches. As a result we at Fermilab are very sensitive to the transmission of beams through transition and become worried when we see behavior such as that shown if Figure 6.

Preservation of longitudinal emittance through transition is also important in other machines. For example, all heavy ion beams will pass through transition in RHIC. Due to the finite crossing angle in that machine the luminosity depends critically on the bunch length, i.e. the longitudinal emittance. In KAON Factories preservation of longitudinal phase space density in itself is not of overwhelming importance, however, acceleration of very large beam intensities with minimal beam loss is. Uncertainties in the ability to accelerate large quantities of beam through transition efficiently have led the TRIUMF people to propose a scheme in which beams never pass through transition within the complex.

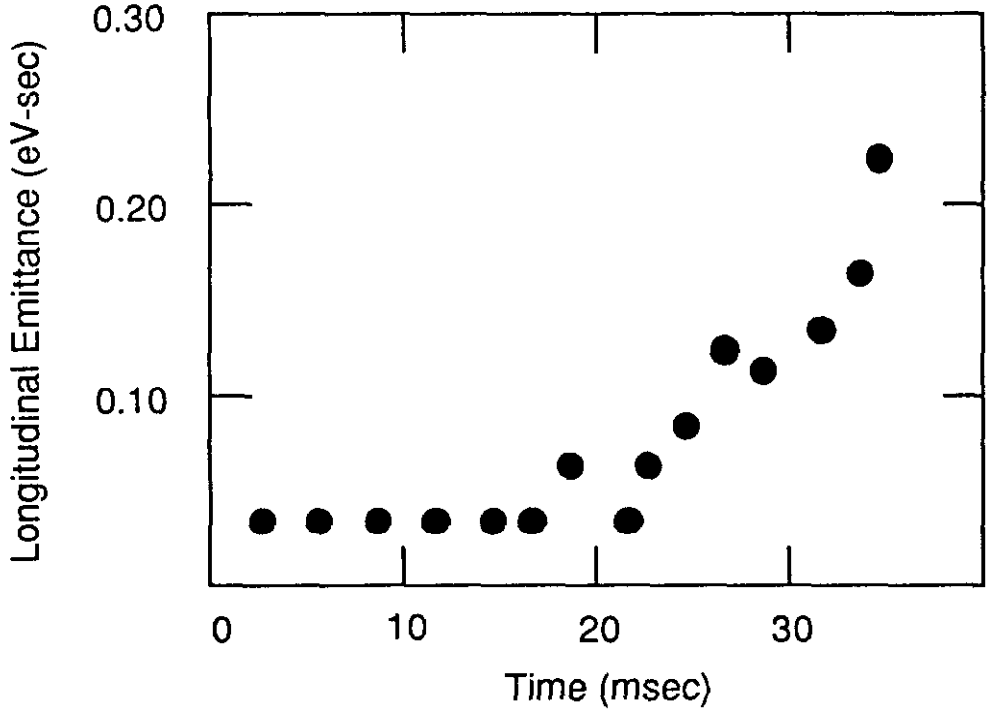

Figure 6: Longitudinal beam emittance as a function of time during the Fermilab Booster acceleration cycle. The beam intensity is about 2×10^{10}/bunch. Transition occurs at about 19 msec.

3.1 Consequences of Transition

Let us start by defining transition. Transition is related to the variation in revolution periods acquired by particles having different momentum offsets relative to the nominal beam momentum. Two effects come into play here--the change in path length, and the change in velocity with momentum:

$$\frac{\Delta T}{T} = \frac{\Delta C}{C} - \frac{\Delta \beta}{\beta}.$$

We will write the pathlength for a particle to complete one revolution of the accelerator as,

$$\frac{\Delta C}{C_o} = \alpha_o \delta + \alpha_1 \delta^2 + \ldots \qquad (4)$$

where $\delta = \Delta p/p_o$ is the momentum offset relative to the central momentum, p_o, and C_o is the pathlength corresponding to p_o. The parameters α_o and α_1 are related to the optics of the accelerator lattice. Note that

$$\alpha_o = \left. \frac{dC/C}{dp/p} \right|_{\delta=0}$$

is also known as the *momentum compaction*. The transition gamma is defined in terms of the momentum compaction and is related to the dispersion and mean radius of the accelerator by,

$$\gamma_t \equiv \frac{1}{\sqrt{\alpha_o}} = \sqrt{\frac{R}{\langle \eta_H \rangle}}.$$

Here R is the mean radius and $\langle \eta_H \rangle$ is the average dispersion in the dipole magnets. The change in speed can be easily worked out and is given by,

$$\frac{\Delta \beta}{\beta} = \frac{1}{\gamma^2} \left(\frac{\Delta p}{p} \right).$$

So, our final result is,

$$\boxed{\frac{\Delta T}{T} = \left(\frac{1}{\gamma_t^2} - \frac{1}{\gamma^2} \right) \left(\frac{\Delta p}{p} \right)}$$

The quantity multiplying $\Delta p/p$ is called the *phase slip factor*, η. As the beam is accelerated through transition η changes sign, attaining the value $\eta=0$ when $\gamma=\gamma_t$.

There are several well-known consequences of crossing through transition. These include:

1. $\phi_s \rightarrow \pi - \phi_s$. The stable synchronous phase moves from one side of the rf wave to the other.

2. $\Delta p/p \rightarrow \infty$. The momentum spread in the beam gets large.

3. $\sigma_L \rightarrow 0$. The bunch length gets short.

4. $f_s \rightarrow 0$. The synchrotron frequency goes to zero.

5. $A_{Bucket} \rightarrow \infty$. The rf bucket area gets large.

None of the above listed consequences directly interferes with the acceleration of beam through transition in circular accelerators. It is common practice to flip the phase of the rf at transition to deal with 1. and to accelerate quickly so that 2. is never attained. The consequences of 1.-5. are not entirely benign, however, when one accelerates substantial quantities of beam through transition.

3.1.1 Microwave Instability

The longitudinal microwave threshold for a Gaussian bunch is given by[13],

$$Z_{\|}/n \leq \frac{2\pi|\eta|(E/e)}{I_p}\left(\frac{\sigma_E}{E}\right)^2. \qquad (5)$$

Here I_p is the peak current in the beam ($eN/\sqrt{2\pi}\sigma_t$ for a Gaussian bunch). As can be seen from the formula, the threshold impedence goes to zero as the Landau damping disappears at transition. This is shown graphically in Figure 7 where the threshold limit is given for the Fermilab Main Injector parameters as a function of time during the acceleration cycle.

Fortunately the expression (5) is derived only for a non-accelerating beam, i.e. $\dot{\gamma}=0$. A more general expression has been derived by J. Wei[14] for the case of a parabolic charge distribution and $\dot{\gamma} \neq 0$:

$$Z_{\|}/n \leq \frac{3V_{rf}\cos\phi_s}{8hI_p}L_\phi^2.$$

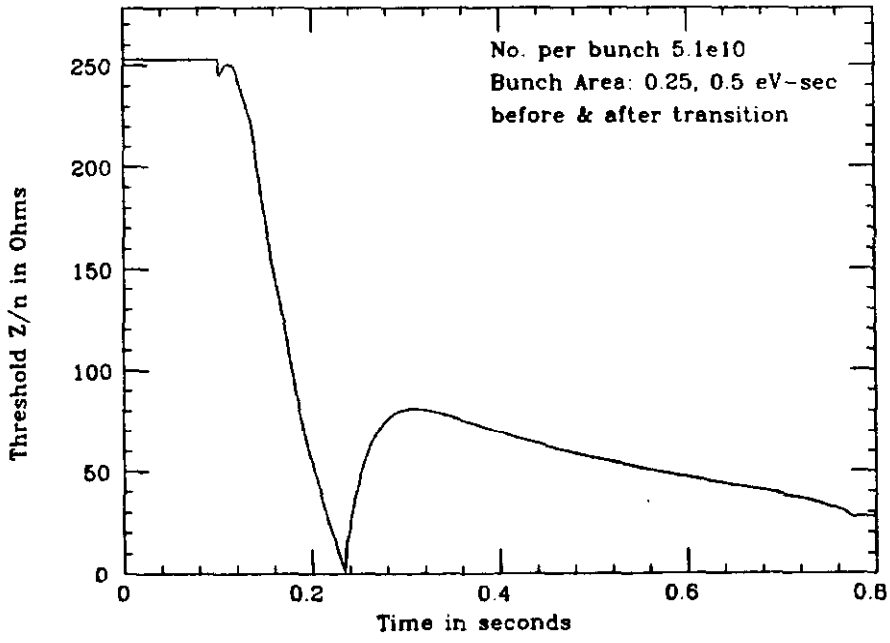

Figure 7: Longitudinal microwave instability threshold as a function of time in the Fermilab Main Injector acceleration cycle. Transition is at about .24 seconds. Parameters used are 5×10^{10} protons/bunch, 0.25 eV-sec bunch area before transition, 0.5 eV-sec after.

Here h is the harmonic number and L_ϕ is the bunch length in radians. For the Fermilab Main Injector the limit here is 10Ω, not the 0Ω indicated by Equation (5). The microwave instability at transition could become a problem if bunch intensities of order 5×10^{11} were ever realized in the Main Injector.

3.1.2 Non-adiabatic Time

As the beam approaches transition η approaches 0, which means that the particles become locked into a particular phase relative to the rf wave. As a particular consequence, close to transition the particles constituting the bunch cannot follow as the rf bucket shape changes rapidly. This results in a so-called *non-adiabatic time* during which the concept of an rf bucket has no meaning. This concept was recognized in the very early days by Courant and Snyder[15]. The non-adiabatic time is given by,

$$T_{na} = \left(\frac{\pi \beta_t^2 \gamma_t^3}{h \omega_0^2 \dot{\gamma}} \frac{E_1/e}{V_{rf} \cos\phi_s} \right)^{1/3} \qquad (6)$$

In the Main Injector the non-adiabatic time will be about 2.0 msec.

3.1.3 Johnsen Effect

The Johnsen effect arises from the chromatic non-linearity represented by a non-zero α_1 in equation (4). We will write down the expression for the transition gamma of different particles in the beam to second order in δ. In doing so we need be careful to make sure we are always defining γ_t in terms of local derivatives, rather than differences from the nominal circumference, C_O:

$$\frac{1}{\gamma_t^2(\delta)} = \frac{p}{C}\frac{dC}{dp}.$$

After taking appropriate derivatives and some algebra, we obtain the expression for the variation of γ_t with δ:

$$\gamma_t(\delta) = \gamma_t(0)\left(1 - \frac{1}{2}\left(1 + \frac{2\alpha_1}{\alpha_O} - \alpha_O\right)\delta\right).$$

The variation of γ_t over the particles making up the beam, coupled with their different energies, means that all particles within the beam do not cross transition at the same time. We will define the *Johnsen*[16] or *non-linear time* as the time difference between the passage through transition of a particle at $\delta=0$, and a particle at $\delta=\sigma_p/p$. You can work it out for yourself and will find,

$$\boxed{T_J = \frac{\gamma_t(0)\left(\frac{3}{2} + \frac{\alpha_1}{\alpha_O} - \frac{\alpha_O}{2}\right)}{\dot{\gamma}}\left(\frac{\sigma_p}{p}\right)} \qquad (7)$$

In the Main Injector the non-linear time will be about 2.7 msec.

A problem in the transmission of beams through transition can arise if the non-linear time is larger than the non-adiabatic time. In this case some particles in the beam will be above, while others will be below, transition for a period of time during which the motion of particles in phase space is describable by the standard set of trajectories, i.e. some particles will be found on bounded and others on unbounded trajectories. This situation will persist until the non-adiabatic time is entered and the particles become locked onto a certain rf phase. The ultimate evolution of the distribution is shown in the simulation[17] of Figure 8.

Wei[14] has given a semi-analytic description of the emittance dilution arising from the Johnsen effect. He finds that the emittance dilution can be parameterized approximately as,

$$\frac{\Delta\varepsilon}{\varepsilon} = \begin{cases} .76 T_J/T_{na} & T_J << T_{na} \\ e^{4/3(T_J/T_{na})} - 1 & T_J > T_{na} \end{cases}$$

For the Main Injector the formula predicts emittance growth of about a factor of five, in reasonable agreement with the simulation. The Johnsen effect is expected to be the dominant mechanism for longitudinal emittance dilution through transition in the Main Injector.

3.1.4 Space-Charge (Bunch shape mismatch)

For intense beams longitudinal space-charge forces can distort the rf waveform over the length of the bunch. The effect is a loss of longitudinal focussing below transition and a gain above. (The effect is the same as that described by Hoffman[18] except that the space-charge associated impedence is capacitive rather than inductive.) The change in longitudinal focussing as the beam passes through transition is accompanied by a change in the rf bucket area. If the change in bucket area is significant the mismatch between the bunch and bucket shapes will cause dilution of the longitudinal phase pace. The mismatch is proportional to the ratio of the self-field of the beam to the externally applied rf voltage. An approximate formula is given by Wei for a parabolic distribution,

$$\frac{\Delta\varepsilon}{\varepsilon} = \frac{2hI_p|Z_{\|}/n|}{V_{rf}\cos\phi_s\, L_\phi^2}$$

where the space-charge impedence is given by,

$$Z_{\|}/n = \frac{ig_0 Z_0}{2\beta\gamma^2} \quad .$$

Here g_0 is a geometric factor (≈ 4) and Z_0 is the impedence of free space ($1/\varepsilon_0 c = 377\Omega$). Note the presence of the same $\beta\gamma^2$ in the denominator as in the transverse space-charge expression (3). For intensities characteristic of the Main Injector this effect is small. However it could become significant if the intensity were to be increase a factor of 5 or so.

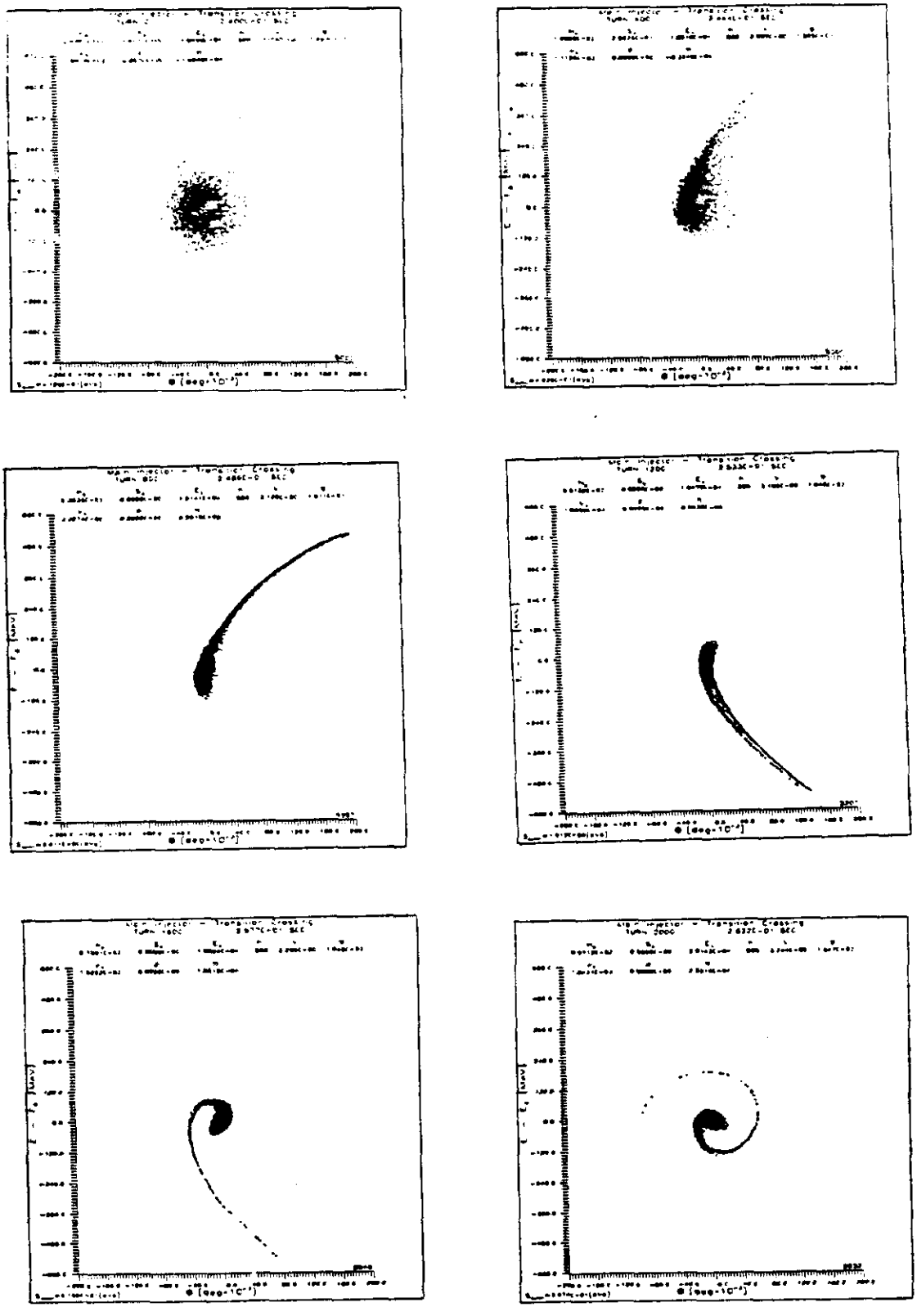

Figure 8: Simulation of the longitudinal phase space for transition crossing in the Main Injector with a 0.4 eV-sec bunch. Time progresses from left-to-right and top-to-bottom. Transition is crossed between the second and third frame. For this example $\alpha_0 = 2.5 \times 10^{-3}$ and $\alpha_1 = 5 \times 10^{-3}$.

3.1.5 Umstätter Effect

The final effect we will consider for high intensity beams is connected with the transverse space-charge described earlier. The change in betatron tune given in (3) is accompanied by a change in γ_t. Particles at the head of the bunch will see a higher γ_t than those at the center. As in the case of the Johnsen effect all particles do not cross transition at the same time, and a "non-linear" time can be defined[19]. This time is proportional to,

$$T_{Umstatter} \propto \frac{N_p}{\dot{\gamma}\,\beta^2\gamma_t^3}$$

and is small compared to the Johnsen time in the Main Injector. As in the case of the longitudinal space charge the Umstätter effect would only become appreciable if the intensity in the Main Injector were to increase to $\sim 3\times10^{11}$/bunch.

3.2 Strategies for Coping with Transition

A number of strategies have been conceived of to ameliorate the effects of transition crossing in circular accelerators. The most straightforward approach usually involves accelerating through transition as quickly as possible so that the effects described above don't have time to come into play. The basic limitation here is the availability of rf accelerating voltage. A second simple approach involves tailoring the rf voltage program through transition in a manner which trades off the various effects listed above. This is generally done empirically on existing machines. However, a number of more sophisticated measures can be taken when an accelerator is still in the design stage.

3.2.1 Transition Jump

One way to increase the effective acceleration rate through transition is to implement a system of pulsed quadrupole magnets in the accelerator which will instantaneously change the optics of the ring in such a manner that the tunes stay fixed, but γ_t drops as transition is approached. This is shown schematically below. Such schemes are implemented in the Fermilab[20] and CERN PS Boosters. Typically γ_t is dropped by one unit in 100 μsec, resulting in an effective $\dot{\gamma}$ of 10000/sec. This represents an increase of a factor 10-100 in $\dot{\gamma}$, and reduces the associated non-linear times by a corresponding amount. In addition, the longer bunches maintained by not allowing the beam to get too close to transition during the adiabatic period minimize effects which are proportional to peak currents such as the microwave instability and space-charge. The downside of

these schemes are that they typically introduce a large dispersion wave into the lattice, precisely at the time when the momentum spread is getting large.

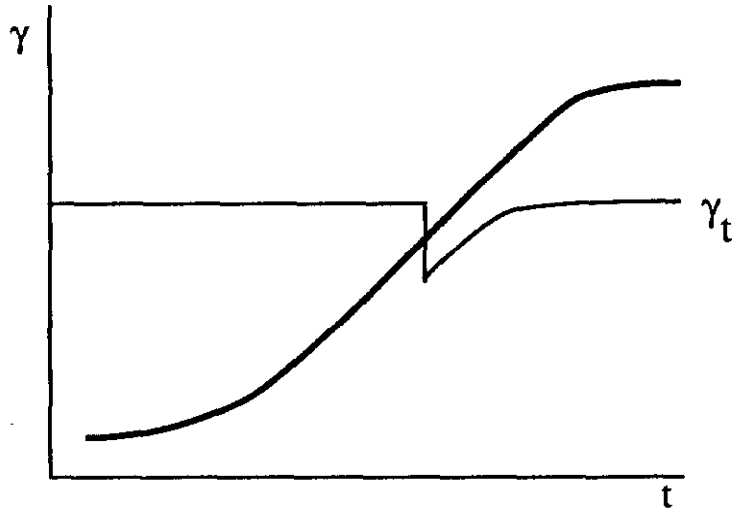

3.2.2 Transition Avoidance

Avoiding transition by removing γ_t from the acceleration range obviously solves the problems described above. The most straightforward way to do this is to design the accelerator so that the transition energy lies either below the injection energy of above the extraction energy. This condition is met in most high energy hadron accelerators and in all existing electron machines. However, since FODO cell based lattices exhibit approximate equality between γ_t and the horizontal tune, hadron accelerators in the 5-20 GeV range often cannot be designed to avoid transition in a natural manner.

One approach which has been investigated is the use of different types of lattices cells to produce a γ_t which is imaginary. (An imaginary γ_t simply means that the average value of the dispersion is less than zero.) Such lattices have been examined as potential designs for the Fermilab Main Injector[21], for the TRIUMF KAON Factory[22], and for the SSC Low Energy Booster[23]. An example of a cell for a possible Main Injector design is shown in Figure 9. The idea is to create negative dispersion by providing a dipole free straight section with something on the order of 150^{o} of phase advance.

The scheme shown in the figure does a good job of keeping the maximum dispersion and beta functions low while not creating abnormal chromaticities. It has the disadvantage of a relatively low dipole packing factor, 53% in this example, and a variety of quadrupole strengths. Further work at Fermilab has indicated that packing factors approaching 67% might be attained with this scheme.

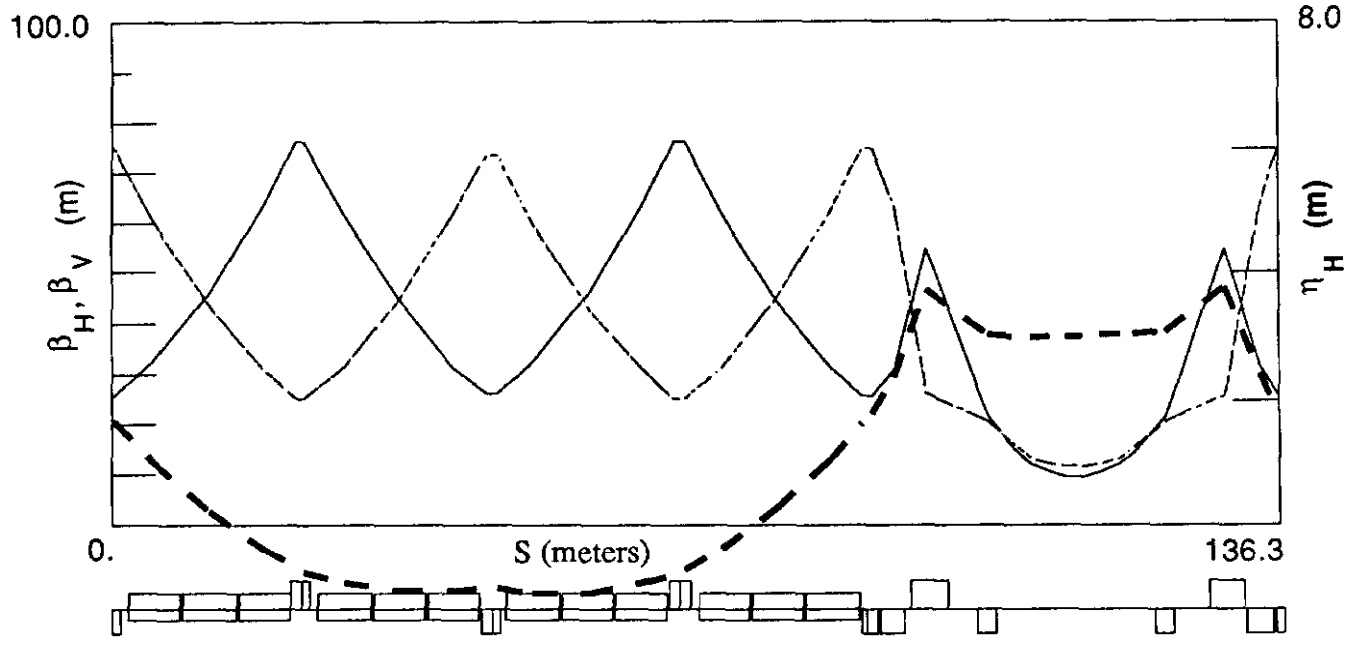

Figure 9: A cell which will produce an imaginary γ_t (39i). The phase advance across the cell is 257^o. Twenty-four such cells could be used to construct the 150 GeV Main Injector. Note, the negative average dispersion through the dipoles.

3.2.3 α_1 Control

You may have noted when we wrote down equation (7) that for $\alpha_1 = -\frac{3}{2}\alpha_o$ the non-linear time is approximately zero. So, one can contemplate eliminating the Johnsen effect by designing a lattice with the appropriate α_1. As you might expect, the value α_1 depends on the distribution of sextupole fields within the ring. Peggs and Bogacz[24] have derived an analytic expression for α_1 as a function of sextupole strength in a FODO cell. A comparison between the analytic prediction and a simulation using the program MAD is given in the table below.

(f,g)	$\alpha_o(x10^{-3})$		$\alpha_1(x10^{-3})$	
	predicted	simulated	predicted	simulated
(0,0)	2.956	2.956	3.213	3.332
(1,0)	2.956	2.956	0.129	0.244
(1,5)	2.956	2.956	-0.638	-0.512

In the table "f" represents the strength of two families of chromaticity correcting sextupoles located at the F and D quadrupoles, while "g" represents

the strength of a third sextrupole at the half-cell midpoint. The point (0,0) has all sextupoles turned off. The point (1,0) has the horizontal and vertical chromaticities adjusted to zero with the third sextupole family off. Finally, (1,5) represents the correction of horizontal and vertical chromaticities with the third sextupole running at five times the strength of the chromaticity sextupoles.

As can be extrapolated from the table, the third sextupole family would be required to run about a factor of 12 higher than the chromaticity correcting sextupoles in order to attain $\alpha_1=-\frac{3}{2}\alpha_0$. However, Peggs and Bogacz have found that the introduction of a small modulation of η_H around the ring can reduce the required strength of the third sextupole family by about a factor of ten. This technique is being pursued at Fermilab and may be incorporated into the Main Injector design.

3.2.4 Higher Harmonic Cavity

Griffin and MacLachlan at Fermilab have suggested the use of a higher harmonic cavity[25] in both the existing Main Ring and in the proposed Main Injector as a means of flattening the rf voltage wave form around transition. In the proposed implementation a second harmonic cavity is turned on at the beginning of the non-linear time and the sychronous phase is simultaneously switched to 90°. This scheme offers two distinct advantages: First, it keeps the bunches long, and I_p low, reducing susceptibility to the micorowave instability and space-charge effects. And second, it combats the Johnsen effect by providing all particles with the same voltage during the non-linear and non-adiabatic times.

A simulation using the program ESME is shown in Figure 10. The simulation is done for the nominal Main Injector parameters and includes longitudinal space-charge as well as an external impedence with $Z/n=5\Omega$ centered at 1.7 GHz. For the case shown the emittance dilution is 2% with $N_p=6\times10^{10}$/bunch and $\alpha_1=3\times10^{-3}$! This technique obviously shows great promise for transmission of high intensity beams through transition.

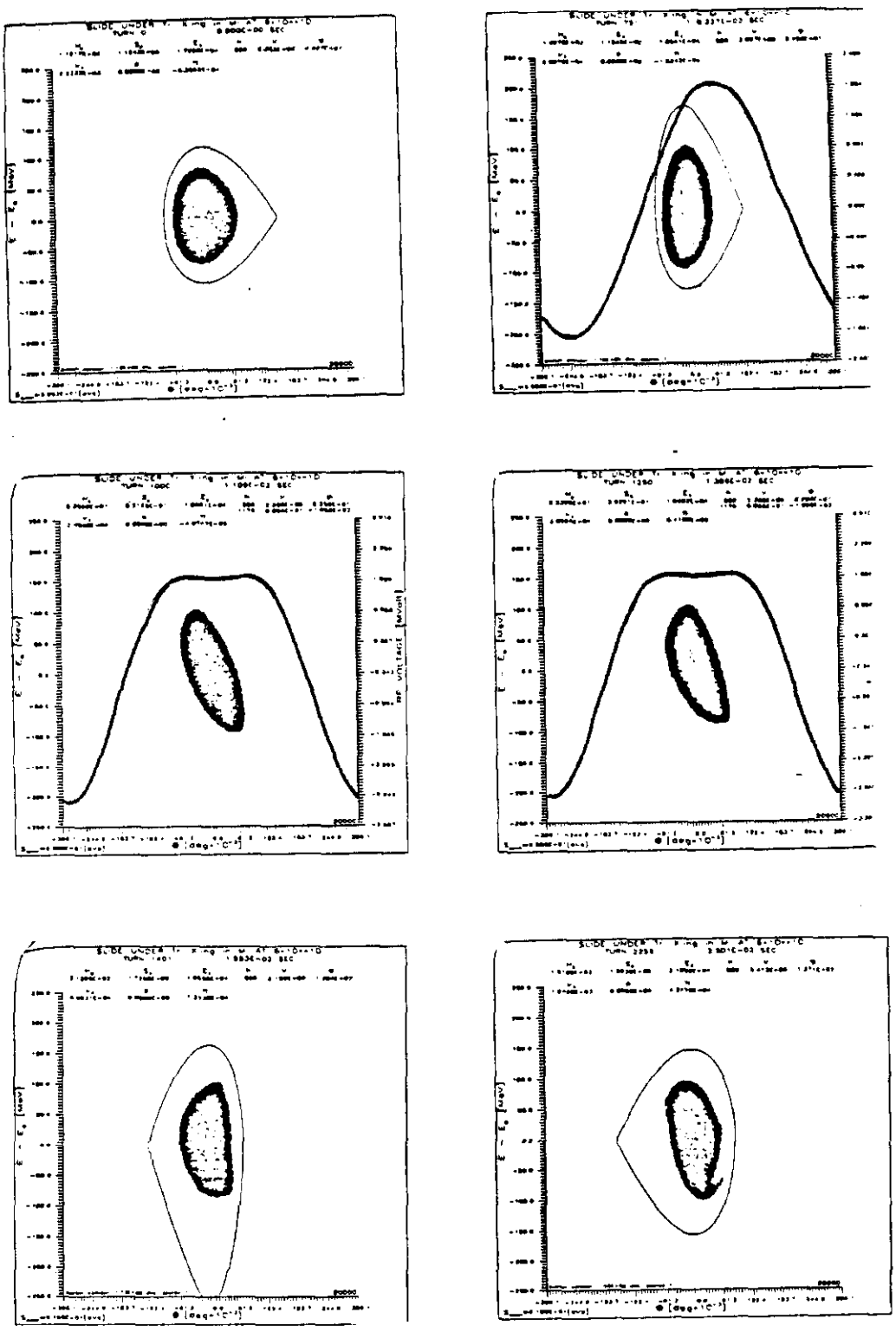

Figure 10: ESME simulation of transmission of beam through transition in the Main Injector using a second harmonic (106 MHz) cavity. The number of protons/bunch is 6×10^{10} with a longitudinal emittance of 0.5 eV-sec. The rf voltage wave form is shown during the period that the second harmonic cavity is on.

4. Summary

Particle intensities, N, and densities, N/ε, emanating from circular accelerators can be limited for $\gamma << \infty$. Limits occur in both transverse and longitudinal phase space. These effects are generally present only in proton and heavy ion accelerators/storage rings.

The primary limit to the transverse densities achievable in a low energy hadron accelerator is due to space-charge forces at injection. Values of the Laslett tune shift parameter achieved in existing accelerators range from 0.4 to 0.9. Our understanding of the phenomona is still rudimentary but developing rapidly with the help of simulations. This limit affects essentially all hadron accelerator complexes. The cures include raising injection energies, increasing the degree of cascading in the complex, and lengthening the bunches.

Transition crossing represents an important limitation in the achievement of high longitudinal phase space densities in circular accelerators. A variety of effects need to be contended with while passing through transition including, the microwave instability, space-charge, and the Johnsen effects. The former are exacerbated by the tendency of the bunch length to approach zero, accompanied by a loss of Landau damping as transition is approaced. Transition crossing impacts essentially all proton accelerator complexes, and even the high energy storage ring RHIC. Potential cures include avoidance, γ_t jumps, α_1 control, and higher harmonic cavities.

References

1. R. Bruce Miller, "Low Energy Beams in Linear Structures", contribution to these proceedings.

2. T. Wangler, "High Brightness Injector", contribution to these proceedings.

3. L. Evans, "Hadron Collider Luminosity Limitations", contribution to these proceedings.

4. C. Ankenbrandt and S.D. Holmes, "Limits on the Transverse Phase Space Density in the Fermilab Booster", Proceeding of the 1987 IEEE Particle Accelerator Conference, 1066, Washington, D.C. (1987).

5. L.J. Laslett, "On Intensity Limitations Imposed by Transverse Space-Charge Effects in Circular Accelerators", Proceedings of the 1963 Summer Study on Storage Rings, BNL-7534, 324, Brookhaven National Laboratory (1963).

6. L. Evans, "Beam Effects in Hadron Colliders", Physics of High Energy Particle Accelerators, AIP Conference Proceedings No. 127, 243 (1985)

7. I. Hofmann and K. Beckert, "Resonance Crossing in the Presence of Space Charge", IEEE Transactions on Nuclear Science, **NS-32** No.5, 2264 (1985).

8. M. Furman, "Effect of the Space-Charge Force on Tracking at Low Energy", Proceedings of the 1987 IEEE Particle Accelerator Conference, 1034, Washington, D.C. (1987).

9. G. Parzan, Nuclear Instruments and Methods, **A281**, 413 (1989).

   G. Parzan, "The Effects of the Intrinsic Space Charge Resonances on the Space Charge Limit", BNL-44562, Brookhave National Laboratory (1990).

10. S. Machida, "Space Charge Effects in Low Energy Synchrotrons", submitted to the 2nd European Particle Accelerator Conference, Nice, France (1990).

    S. Machida, "Space Charge Effects in Low Energy Proton Synchrotrons", University of Tokyo/Texas Accelerator Center PhD. Thesis (1990).

11. S.R. Mane, "Space-Charge Effects in the Fermilab Main Ring at 8 GeV", Proceedings of the 1989 IEEE Particle Accelerator Conference, 1804, Chicago, Il. (1989).

12. J. Rosensweig and P. Zhou, "Envelope Instability in Low Energy Proton Synchrotrons", Fermilab FN-539 (1990).

13. S. Krinsky and J.M. Wang, Particle Accelerators, **17**, 109 (1985)

14. J. Wei, "Longitudinal Dynamics of the Non-Adiabatic Regime on Alternating Gradient Synchrotrons", State University of New York at Stony Brook PhD Thesis (1990).

    J. Wei, "Transition Crossing in the Main Injector", Proceedings of the Fermilab III Instabilities Workshop, Fermilab TM-1696 (1990).

15. E.D. Courant and H.S. Snyder, Ann. Phys., **3**, 1 (1958)

16. K. Johnsen, Proceedings of CERN Symposium on High-Energy Accelerators and Pion Physics, **Vol. 1**, 106, Geneva (1956).

17. A. Bogacz, "Transition Crossing in the Main Injector - ESME Simulation", Proceedings of the Fermilab III Instabilities Workshop, Fermilab TM-1696 (1990).

18. A. Hoffman, "Coherent Beam Instabilities", contribution to these proceedings.

19. A. Sørenssen, Particle Accelerators, **6**, 141 (1975)

20. W. Merz, C. Ankenbrandt, and K. Koepke, "Transition Jump system for the Fermilab Booster", Proceedings of the IEEE Particle Accelerator Conference, 1343, Washington, D.C. (1987)

21. D. Trbojevic, "Design Method of a High Energy Accelerator without Transition", submitted to the 2nd European Particle Accelerator Conference, Nice, France (1990).

22. TRIUMF-KAON Project, "KAON Factory Study-Accelerator Design Report", TRIUMF, Vancouver, B.C. Canada (1990)

23. R. Gerig, Private Communication

24. A. Bogacz and S. Peggs, "Comments on the Behavior of α_1 in the Main Injector γ_t Jump Schemes", Proceedings of the Fermilab III Instabilities Workshop, Fermilab TM-1696, (1990).

25. J. Griffin and J. MacLachlan, abstract submitted to the 1991 IEEE Particle Accelerator Conference, San Francisco, Ca.